Digital Keywords

707 Military Derivative Airplane
Airplane Bank Angle Modulation
Computer Simulation
Control System
CFM56 Engine
E-6 Airplane
EASY5
Fuzzy Logic
Long Trailing Wire Antenna (LTWA)
Reduced Pilot Workload
Robert G. Borst
TACAMO Mission
Wind Shear Induced Oscillation
Yoyo Oscillation

AIAA-93-3868-CP

Fuzzy Logic Control Algorithm for Suppressing E-6A Long Trailing Wire Antenna Wind Shear Induced Oscillations

Robert G. Borst*, Glen F. Greisz†, and Allen G. Quynn†
Boeing Defense & Space Group, Electronics Systems Division, Air Vehicle Technology
Seattle, Washington

The E-6 mission requires deployment of approximately five miles of Long Trailing Wire Antenna (LTWA) and maintaining it nearly vertical to conduct Very Low Frequency (VLF) radio communication with the Navy ballistic missile submarine fleet. To accomplish this mission, the E-6 aircraft flies an "orbit" profile characterized by slow airspeeds and high bank angles with the principal objective of maximizing LTWA verticality. Wind shear present in the surrounding air mass produces an undesirable "yoyo" altitude oscillation in the end of the LTWA. A LTWA model and fuzzy logic control algorithm were developed and evaluated. The fuzzy logic control algorithm was found to be very effective in suppressing the LTWA yoyo oscillation. The results of this development effort are presented.

Nomenclature

Definitions

DBA	Delta Bank Angle
i	i^{th} wire segment where i=1 to N, starting with the wire segment closest to the aircraft(towpoint).
LTWA	Long Trailing Wire Antenna
OLC	Open Loop Correlation
RHA	Reference Heading Angle
WT	LTWA Wire Tension

Constants

C_N	=Normal force coefficient(1.0) for LTWA
C_D	=Friction drag coefficient for LTWA
D	=LTWA diameter, feet
G	=Gravity vector (-32,0,0), ft/sec2
$h_{airplane}$	=Airplane altitude, feet
L_{LTWA}	=Total length of LTWA, feet
m	=Mass of each of the uniform LTWA wire segments except the last(bottom) one, slugs
m_N	=Mass of the last LTWA segment, wire plus drogue mass, slugs
N	=Number of uniform LTWA segments
S	=Length of an LTWA segment between any two mass points, feet

Variables

A_{CUE}	=WT amplitude cue value, lbs
DBA	=Delta Bank Angle, degrees
F_{A_i}	=Aero force vector on mass segment i, assumed to act on mass m, lbs
F_{D_i}	=Drag force vector on i^{th} mass segment of LTWA, lbs
F_{N_i}	=Normal force vector on i^{th} mass segment of LTWA, lbs
h_{drogue}	=Drogue(lower end of LTWA) altitude, feet
$INPUT_j$	=j^{th} input to DBA fuzzy controller
M_{DBA}	=Magnitude factor on DBA update, output of fuzzy controller
$OUTPUT_j$	=j^{th} output from DBA fuzzy controller
SGN_{DBA}	=Sign factor for DBA update, output of fuzzy controller
T_i	=LTWA tension scalar between the i^{th} and $(i-1)^{st}$ mass segments, lbs
V_{R_i}	=Velocity vector of the i^{th} mass point, relative to the wind, ft/sec
VERT	=Verticality of LTWA, percent
V_{N_i}	=Velocity vector normal to the i^{th} LTWA segment, relative to the wind, ft/sec
X_i	=Position vector of the i^{th} mass segment, (3 components: up, east, north), feet
X_0	=Position vector of the aircraft towpoint, feet
ΔX_i	=Vector difference between X_i and X_{i-1}, feet
Ψ_{CUE}	=WT heading cue value, degrees

Presented as Paper 93-3868 at AIAA Guidance, Navigation, and Control Conference, Monterey, CA, August 9-11, 1993.

*Acting Flight Controls Supervisor. Senior Member, AIAA.
†Flight Controls Engineer.

Introduction

THE Boeing Company is under contract with the US Navy to develop the E-6 aircraft for TACAMO missions. The E-6, a derivative of the Boeing 707 airframe, is a land-based, subsonic aircraft incorporating modifications necessary to satisfy the Navy mission requirements. The E-6 mission requires deployment of approximately five miles of Long Trailing Wire Antenna (LTWA) to conduct Very Low Frequency(VLF) radio communication with the Navy ballistic missile submarine fleet. To accomplish this

mission, the E-6 aircraft flies an "orbit" profile characterized by slow airspeeds (10 KEAS above stall buffet) and high bank angles (as large as 50 degrees) with the principal objective of maximizing and stabilizing LTWA verticality.

Wind shear present in the surrounding air mass produces an undesirable "yoyo" altitude oscillation in the end of the LTWA. Yoyo suppression can be accomplished by choosing an appropriate anti-yoyo maneuver which consists of modifying the nominal orbit bank angle as a function of aircraft heading angle. The use of a rule-based fuzzy logic control algorithm to calculate and update the anti-yoyo maneuver parameters was motivated by nonlinear LTWA behavior and lack of a well-defined input/output relationship.

There are many publications which describe fuzzy logic theory and rule based systems in detail[1,2]. The concept of fuzzy set theory differs from the classical "crisp" set theory (either hot or cold), by allowing partial membership in a set(hot to degree 0.8, cold to degree 0.2). The degree of membership permitted with the fuzzy approach leads to a set of modified logical relationships which replace those of the crisp theory. During recent years, fuzzy logic has seen increasing use in engineering applications.

A generalized fuzzy logic process is shown in Figure 1. The three major blocks define the flow from crisp inputs to crisp outputs. The first block defines the membership values in each of the sets for each crisp input.

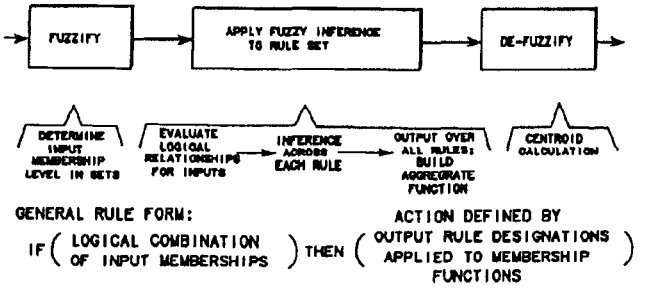

FIGURE 1
FUZZY CONTROL CONCEPT- GENERAL BLOCK DIAGRAM

The second block is the fuzzy controller inference engine. Input memberships are evaluated by applying fuzzy logic to a logical relationship defined for each rule. The result of the input processing can be thought of as a weighting factor for each rule based on the fuzzy set memberships of the inputs. The rules, containing IF/THEN clauses, each infer output memberships. Aggregate functions are then constructed for each output which consist of the weighted contribution from each rule. The third block computes the "centroid" of the calculated aggregate function. This results in a single crisp number for each output variable.

A number of simple illustrative examples are provided in the literature[3,4]. From a control system point of view, a rule based controller is a non-linear processor whose input/output relationship is usually difficult to define in the traditional linearized transfer function sense.

For this application, "sum-min", rather than "max-min" inference was used. This deviates from classical fuzzy rule composition because it allows output membership values greater than unity. However, the de-fuzzification process is insensitive to this conceptual problem. Rules with small weighting factors tend to get neglected in the "max" operation but make a helpful contribution when the "sum" is utilized in this application.

This paper provides an overview of the LTWA analysis model and the fuzzy logic algorithm developed to minimize the effect of the the wind shear induced yoyo oscillations.

The LTWA Oscillation Problem

E-6 orbital flight requires a slow airspeed and high bank angle. When these commands are properly selected, the LTWA "drops in" and assumes a downward spiral orientation. Figure 2 illustrates the E-6 aircraft in orbit with the LTWA deployed. Wind shear(wind speed and direction varying with altitude) acting on the LTWA produces a "yoyo" oscillation as illustrated by the simulation time histories shown in Figure 3. It should be noted that the oscillation is not a result of LTWA elastic behavior, but due to the wind shear forcing function. Consequently, the yoyo oscillation frequency corresponds to the orbit frequency.

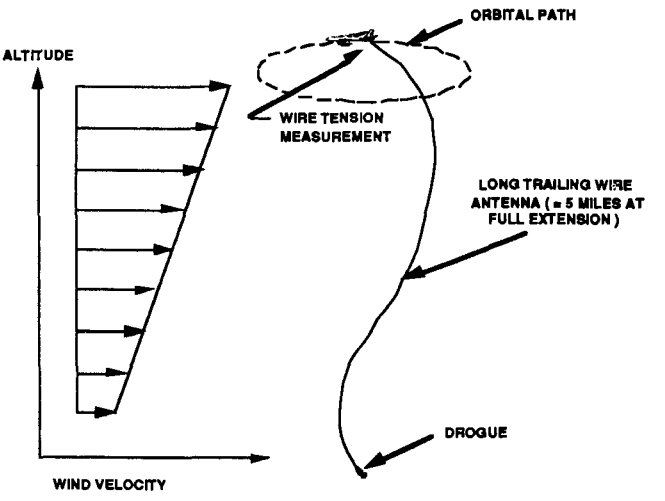

FIGURE 2
WIND SHEAR ACTING ON LONG TRAILING WIRE ANTENNA(LTWA) DURING ORBITAL FLIGHT

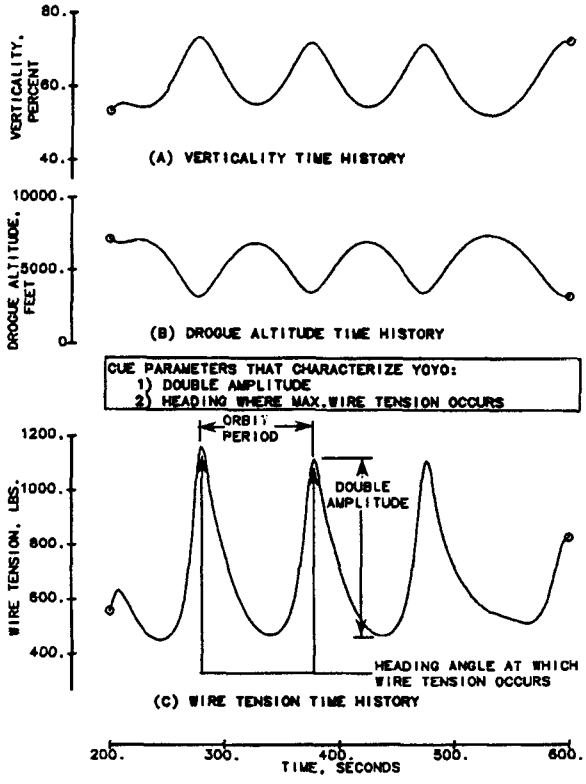

FIGURE 3
TIME HISTORIES SHOWING YOYO OSCILLATIONS - MODERATE WIND SHEAR MAGNITUDE

The LTWA transmission capability is affected by its verticality, defined by eq. (1) in percent. Verticality

$$VERT = \frac{100\,(h_{airplane} - h_{drogue})}{L_{LTWA}} \qquad (1)$$

variations shown in Figure 3(a) are caused by wind-shear induced yoyo and are undesirable. Drogue altitude, shown in Figure 3(b), is sensed and used for evaluating the effectiveness of the anti-yoyo system but is not used by the control system. Wire tension, shown in Figure 3(c), is the primary control system feedback parameter and will be discussed later.

An anti-yoyo maneuver consists of an incremental bank angle superimposed on the nominal orbit bank angle command. Figure 4 shows two such maneuver profiles. A profile is characterized by a Delta Bank Angle (DBA) and a Reference Heading Angle (RHA). DBA is the incremental bank angle magnitude of the maneuver. RHA references the maneuver to an aircraft heading angle to produce the proper maneuver phasing.

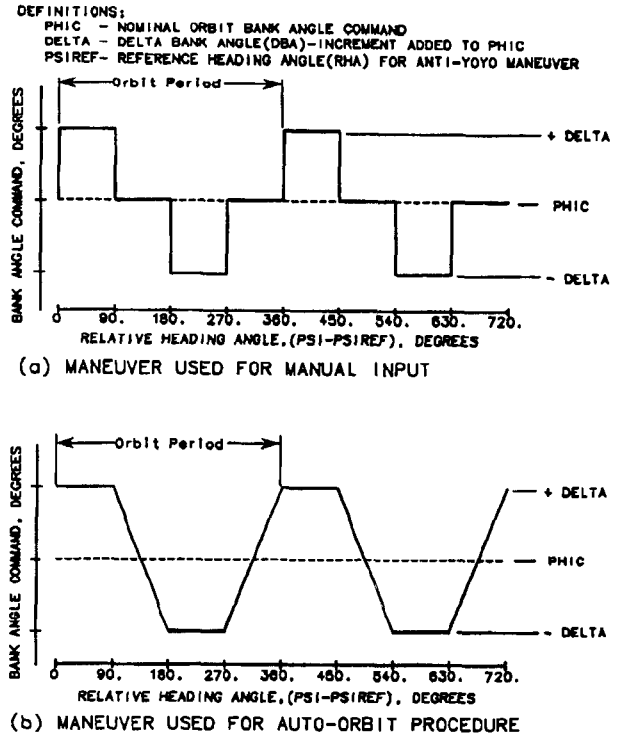

FIGURE 4- ANTI-YOYO MANEUVER PROFILES

The Figure 4(a) anti-yoyo maneuver, which consists of a steep, nominal, shallow, nominal sequence repeated every 360 degrees of heading angle, was used in the past for manual implementation of the procedure. Even for this relatively simple maneuver, the pilot workload is significant. The Figure 4(b) maneuver, more effective per degree of DBA for yoyo suppression, was used for this application.

The LTWA Analysis Model

Auto-orbit performance was evaluated using a simulation which incorporated each element of the orbiting system. The simulation contains models of the physical systems(LTWA wire and airplane) and the auto-orbit software. A relatively simple model of the airplane was used by assuming it to be a point mass towing the wire and flying a constant altitude orbit at the commanded speed. The towpoint acceleration is based on the nominal bank angle command. A first order lag was used to represent the airplane bank angle dynamics.

The LTWA equations of motion are approximated by replacing the wire with a set of N mass points connected by massless lengths of wire, assumed to be inextensible. A passive drogue is attached to the bottom of the LTWA. Inputs to these equations are the wind speed and direction as a function of altitude, and the position, velocity, and acceleration of the tow point.

In the following analysis, all wire segments are the same length, S, and all mass points have the same mass, m, except the bottom one which has a mass of m plus that

of the drogue, and is denoted by m_N. The segment accelerations are given by eq's. (2) and (3).

$$\ddot{X}_i = \frac{F_{A_i}}{m} + \frac{T_i (X_{i-1} - X_i)}{m\ S} + \frac{T_{i+1} (X_{i+1} - X_i)}{m\ S} + G \quad \text{for } i=1,N-1 \qquad (2)$$

$$\ddot{X}_N = \frac{F_{A_N}}{m_N} + \frac{T_N (X_{N-1} - X_N)}{m_N\ S} + G \quad \text{for } i=N \qquad (3)$$

These N second order differential equations in the N state vectors, X_i, constitute the equations of motion. However they cannot be integrated because the tensions, T_i, are not known. However, since the wire segments are inextensible, the length of each one is constant and eq. (4)

$$\dot{S} = \ddot{S} = 0 \quad \text{for } i = 1,N \qquad (4)$$

applies. Expressing $\ddot{S}$ in terms of the X_i and $\dot{X}_i$ results in N simultaneous equations, which are linear in the T_i. They can be solved for the T_i in terms of the known values of X_i and $\dot{X}_i$.

The aero force on the i^{th} wire segment is modelled as the vector sum of two components[5]:

1) a force normal to the wire, F_{N_i}.
2) a drag force, F_{D_i}, acting in a direction opposite to the relative velocity.

Equations (5)-(7) are used to compute the aero force vector, F_{A_i} in terms of the two components, where V_{R_i} is the velocity vector of the i^{th} mass segment relative to the wind. The force on the bottom mass is given by the same equations augmented by the drag on the drogue with appropriate values for C_D and D*S.

$$V_{N_i} = V_{R_i} - \frac{(V_{R_i} \bullet \Delta X_i)\ \Delta X}{S^2} \qquad (5)$$

(A • B is the scalar product of the vectors A and B)

$$F_{D_i} = .5\ \rho\ S\ D\ C_D\ |V_{R_i}|\ V_{R_i} \qquad (6a)$$

$$F_{N_i} = .5\ \rho\ S\ D\ C_N\ |V_{N_i}|\ V_{N_i} \qquad (6b)$$

$$F_{A_i} = F_{N_i} + F_{D_i} \qquad (7)$$

Solution of the equations is facilitated by defining a new variable which is the vector difference between X_i and X_{i-1}, given by eq. (8). In terms of the new variable, eq's (2) and (3) can be rewritten as eq's. (9)-(11) and Eq. (4) can be rewritten as eq. (12). Differentiating twice and setting $\dot{S}=\ddot{S}=0$ yields eq. (13). These N equations are

$$\Delta X_i = X_i - X_{i-1} \quad \text{for } i=1,N \qquad (8)$$

$$\Delta\ddot{X}_i = \frac{F_{A_1}}{m} - \frac{T_1\ \Delta X_1 + T_2\ \Delta X_2}{m\ S} + G - \ddot{X}_0 \quad \text{for } i=1 \qquad (9)$$

$$\Delta\ddot{X}_i = \frac{T_{i-1}\ \Delta X_{i-1} - 2\ T_i\ \Delta X_i + T_{i+1}\ \Delta X_{i+1}}{m\ S} + \frac{F_{A_i} - F_{A_{i-1}}}{m} \quad \text{for } i=2,N-1 \qquad (10)$$

$$\Delta\ddot{X}_N = \frac{F_{A_N}}{m_N} - \frac{F_{A_{N-1}}}{m} + \frac{T_{N-1}\ \Delta X_{N-1}}{m\ S} - \frac{T_N\ \Delta X_N}{S}\left(\frac{1}{m} + \frac{1}{m_N}\right) \quad \text{for } i=N \qquad (11)$$

$$(S)^2 = \Delta X_i \bullet \Delta X_i \qquad (12)$$

$$(\dot{S})^2 + (\ddot{S})(S) = \Delta\dot{X}_i \bullet \Delta\dot{X}_i + \Delta\ddot{X}_i \bullet \Delta X_i = 0 \qquad (13)$$

linear in the N unknown tensions, T_i, and can be easily solved. After the tensions and aero forces are calculated as described above, the equations for $\Delta\ddot{X}$ can be integrated to give the velocity and position of each point as a function of time. These equations account for the effects of wind shear and towpoint motion.

Figure 5 compares measured flight test data and simulation data. The simulation was driven by the same wind profile measured during the flight test. Good agreement is shown for drogue altitude and LTWA wire tension.

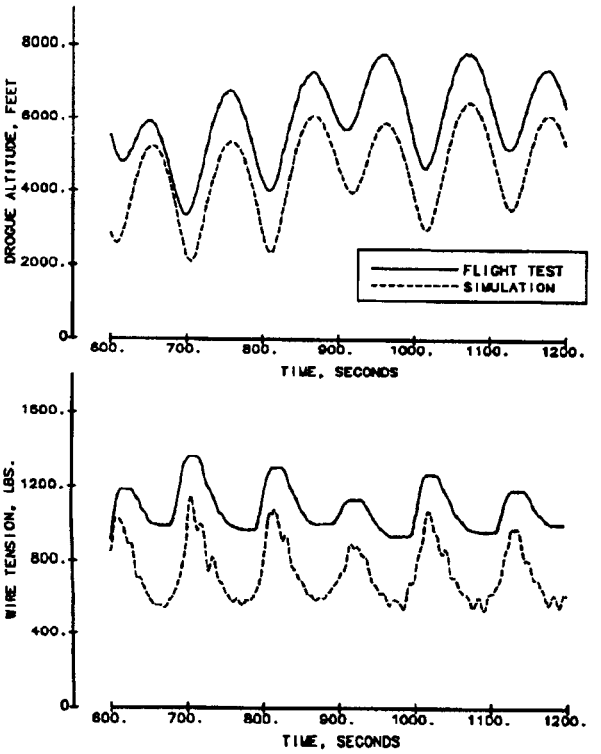

FIGURE 5
COMPARISON OF FLIGHT TEST AND SIMULATION DATA

LTWA Cue Parameter Characteristics

LTWA tension is measured at the towpoint and is the primary control feedback variable. Minimizing the LTWA tension oscillation in turn minimizes the verticality oscillation. Figure 3(c) illustrates the two cue parameters calculated from the LTWA signal to characterize the yoyo:

1) the peak-to-peak oscillation amplitude; a measure of the yoyo magnitude.
2) the aircraft heading angle at which the maximum LTWA tension occurs; a measure of the yoyo phasing.

Prior to anti-yoyo maneuver initiation, the LTWA cue parameters reflect only the wind shear induced yoyo. Once the maneuver is initiated, the cue parameters reflect the residual yoyo produced by the wind shear and the anti-yoyo maneuver. The cue parameters then represent the error vectors shown in Figure 6 and are used to derive the inputs from which updates to the anti-yoyo maneuver are calculated.

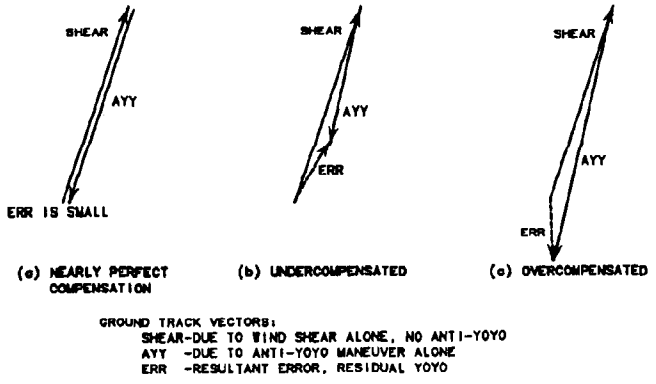

FIGURE 6
GROUND TRACK VECTOR DIAGRAMS SHOWING AFFECT OF ANTI-YOYO MANEUVER

The error vector is illustrated for three cases in Figure 6. The anti-yoyo maneuver may be: a) nearly perfect, b) undercompensated (DBA too small), or c) overcompensated (DBA too large). With nearly perfect compensation, the anti-yoyo maneuver produces a ground track vector which cancels the effective wind shear. By definition, the RHA and DBA are "optimum" in Figure 6(a). The difference between (b) and (c) is primarily one of error vector direction. The error vectors point in opposite directions. This property of phase reversal was used in the rule base to determine the under- or overcompensated condition.

Another characterization of this phase reversal is shown in Figure 7, where the residue cue parameters are plotted as a function of the anti-yoyo maneuver parameter RHA. In Figure 7(a), the amplitude curve reaches a minimum yoyo level at an optimum RHA value of 0 degrees(chosen for illustrative purposes). The constant line represents the amplitude cue value without an anti-yoyo maneuver. For RHA values significantly different from 0 degrees, the residual yoyo amplitude is greater than that with no maneuver. This property was used in the rule base to identify RHA conditions well away from optimum values. Figure 7 shows that RHA values must be fairly close to optimum to achieve the goal of significantly reducing yoyo oscillation amplitude.

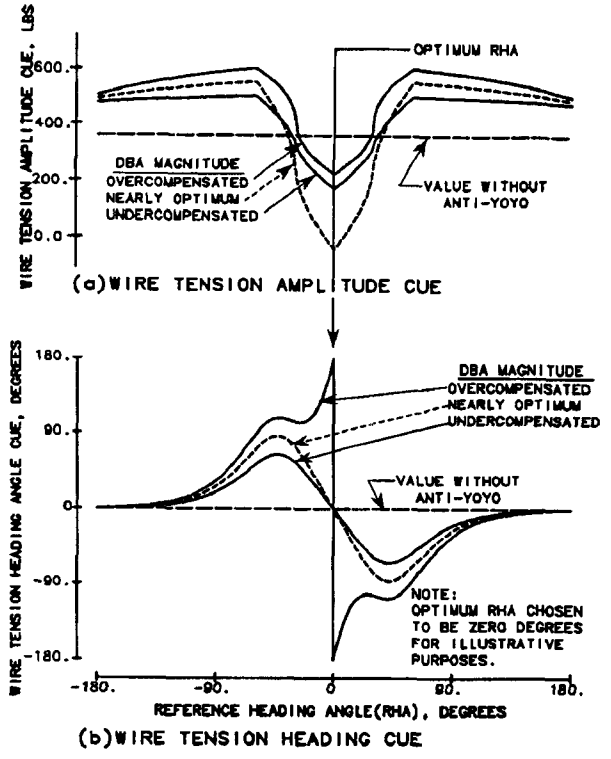

FIGURE 7
CUE CHARACTERISTICS FOR ANTI-YOYO MANEUVER

Figure 7(b) shows the heading cue values resulting from the anti-yoyo maneuver. The constant line again represents the pre-anti-yoyo level. The phase reversal previously discussed for the DBA under- and over-compensated cases is apparent. For the undercompensated case, the residue phase cue is seen to coincide with the pre-anti-yoyo phase cue when RHA is optimum. This relationship was used in formulating the anti-yoyo maneuver rule base.

The LTWA Fuzzy Logic Anti-yoyo Controller

The purpose of the fuzzy logic controller is to calculate anti-yoyo maneuver parameter values, RHA and DBA. By adding the appropriate incremental bank angle to the nominal aircraft orbit bank angle, the LTWA yoyo oscillation is suppressed during the E-6 orbit mission. Inputs to the controller are the LTWA cue parameters. Outputs are RHA and DBA which define the phase and magnitude of the anti-yoyo maneuver shown in Figure 4(b). Rule-based fuzzy logic constructs were chosen to implement parameter selection because of the nonlinear nature of the

controlled system and the lack of a well defined input/output relationship. A block diagram of the closed loop control system is shown in Figure 8.

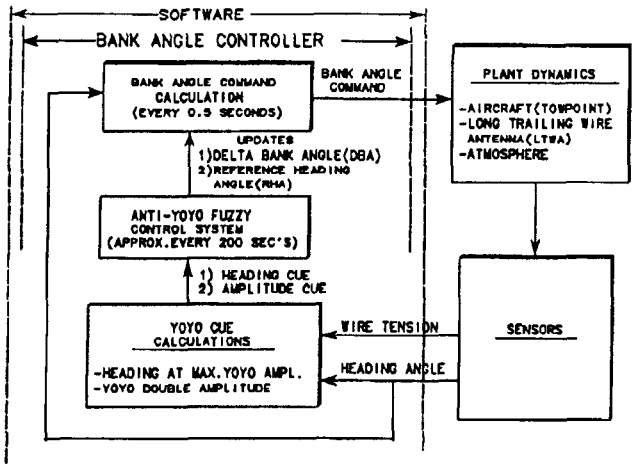

FIGURE 8
CLOSED LOOP ANTI-YOYO CONTROL SYSTEM

To initialize the maneuver parameters, an Open Loop Correlation (OLC) technique is used. Cue values provide the inputs to an algorithm from which the RHA and DBA are calculated. The OLC algorithm is based on simulation results and data obtained from the flight test program conducted on the E-6 aircraft with the LTWA deployed. Simulation results have verified that the OLC algorithm does indeed provide a maneuver close to the optimum for a wide variety of orbit and wind conditions. The RHA has generally been found to be within ± 10 degrees, while the DBA typically is low by 0-20%. The low side bias is permitted because simulation experience has shown the "undercompensated" cue values to be slightly more reliable for use in forming anti-yoyo maneuver updates which converge rapidly to optimum values.

While a properly executed OLC maneuver significantly reduces yoyo amplitude, closed loop corrections by the control system are required to:

1) recover from large error conditions if they occur.
2) further converge to optimum values.
3) track time varying wind shear over an extended period of several hours.

An error condition is defined as the difference between the current maneuver parameters (RHA and DBA) and the optimum values resulting in minimum yoyo amplitude. A functional block diagram of the bank angle controller is shown in Figure 9. The control system software is executed at a basic frame time of 0.5 seconds and performs two functions during each pass:

1) A bank angle command is calculated.
2) The LTWA cue parameters are inspected to see if an anti-yoyo update is required.

The first function combines the nominal orbit bank angle with the anti-yoyo maneuver incremental bank angle schedule(Figure 4(b)) using the current values of RHA and DBA. The result is a bank angle command to the autopilot. The second function initiates an anti-yoyo parameter update every second cue update, roughly equivalent to every second orbit. A typical orbit period is 100 seconds. Simulation results have shown that after an anti-yoyo update is performed, two cue updates are required before the transient settles down and the cue is again a reliable indicator for the next anti-yoyo update.

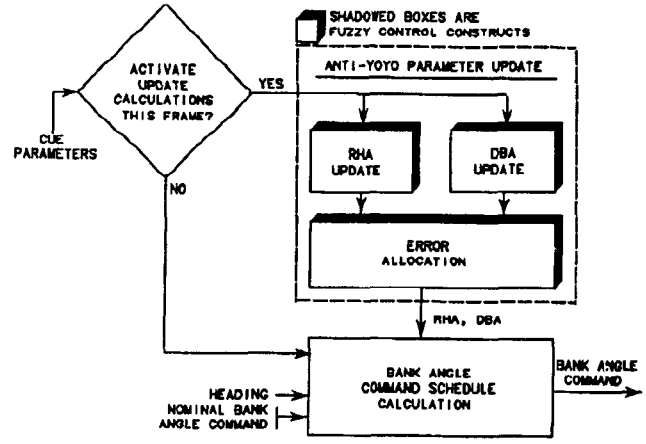

FIGURE 9
ANTI-YOYO FUZZY CONTROLLER

When activated, anti-yoyo parameter updates are calculated within each of the three shadowed fuzzy logic blocks of Figure 9. The RHA Update block calculates a Reference Heading Angle update to the previous value based on inputs formed from updated amplitude and heading cues. Similarly, the DBA Update block updates the DBA. This block will be discussed in greater detail as an example of the fuzzy logic constructs. The Error Allocation block receives the update values for RHA and DBA as inputs together with the cue values and decides how much of each to apply at the current update cycle. This is done because an RHA or DBA update may be a better choice at a particular time. Large simultaneous updates to both parameters tend to confuse cause and effect for the following update cycle two orbits later. When close to optimum, small simultaneous updates provide good convergence.

Figure 10 shows the RHA and DBA Update fuzzy block calculations in general form. The inputs are current cue values from the cue calculation block. Some are stored to form fuzzy inputs for use in later update calculations. After calculating the fuzzy inputs, the fuzzy control blocks are executed to produce an update value.

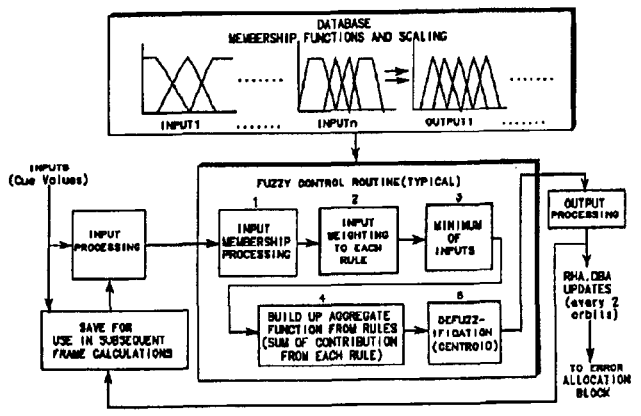

FIGURE 10
FUZZY ALGORITHM FOR DBA, RHA UPDATES, GENERAL FORM

Inputs to the fuzzy controller for the DBA Update block are given by eq's. (14) - (18). They are each derived using current or previous cue values and previous output values. $INPUT_1$ is the last previous value of SGN_{DBA}, an the sign variable and an output from the fuzzy controller. Its use allows rules that generically look like: "if the last update was negative and the yoyo amplitude decreased, the next update should again be negative". $INPUT_1$ has continuous values from -1 to +1, rather than -1 or +1, an example of a "fuzzy", rather than "crisp", formulation. Thus, the sign may be positive, but possibly to a degree less than unity. $INPUT_2$ is a measure of how well the last previous update did and hence, has a similar use to $INPUT_1$ in the "do more of the same" type of rule.

$$INPUT_1 = SGN_{DBA(previous)} \tag{14}$$

$$INPUT_2 = A_{CUE(current)} / A_{CUE(previous)} \tag{15}$$

$$INPUT_3 = A_{CUE(current)} / A_{CUE(pre\text{-}ayy)} \tag{16}$$

$$INPUT_4 = \Psi_{CUE(current)} - \Psi_{CUE(pre\text{-}ayy)} \tag{17}$$

$$INPUT_5 = A_{CUE(current)} \tag{18}$$

$INPUT_3$ is a performance measure of the current amplitude cue relative to the pre-anti-yoyo cue and allows use of conclusions derived from Figures 6 and 7. As the ratio gets small, the "bucket" of Figure 7(a) has been found and updates are reduced accordingly. $INPUT_4$ compares the current heading cue with the pre-anti-yoyo value and is useful in recognizing the 180 phase shift indicative of DBA over- or undercompensation as discussed earlier. $INPUT_5$ recognizes the absolute yoyo value and is useful in dealing with light winds resulting in small yoyo amplitudes. There is no point in making large updates if the yoyo amplitude is relatively small. It should be noted that $INPUT_3$ and $INPUT_4$ are referenced to the pre-anti-yoyo cue values and are very useful in early convergence to the bucket minimum. As the mission progresses, time variations in the wind shear cause rules using these inputs to become less meaningful. The process then becomes one of tracking the minimum, rather than finding it. The solution is to vary the weighting on these rules with time.

The outputs are given by eq's. (19) and (20). $OUTPUT_1$ controls the sign of the correction while $OUTPUT_2$ sets the magnitude. Since the DBA is a magnitude and always positive, the two outputs are combined to either multiply when increasing DBA ($SGN_{DBA} > 0$), or divide when decreasing DBA ($SGN_{DBA} < 0$), as given by Eq. (21).

$$OUTPUT_1 = SGN_{DBA} \tag{19}$$

$$OUTPUT_2 = M_{DBA} \tag{20}$$

$$DBA_{(new)} = DBA_{(previous)} * (1.+ SGN_{DBA} * M_{DBA}) \quad SGN_{DBA} > 0 \tag{21a}$$

$$= DBA_{(previous)} / (1.- SGN_{DBA} * M_{DBA}) \quad SGN_{DBA} < 0 \tag{21b}$$

The membership functions for the five inputs and two outputs are shown in Figures 11 and 12. While the functions are not unusual a couple of practical comments are worthwhile. The "NXL" member in $INPUT_3$ is NOT("XL"). In writing the software, a generic routine was created to solve the fuzzy control logic and it was found to be easier to formulate the IF clauses in terms of AND's and avoid NOT's. Thus, it was easier to define a new member "NXL" rather than perform a fuzzy logic NOT. The "VN" membership range of 0.0 to 2.0 for $OUTPUT_2$ is a departure from classic membership definition. This technique was used to make sure a rule using "VN" would dominate other rules when applied. The de-fuzzification process is not affected by values greater than 1.0.

The DBA Update rule base is shown in Table 1. Both inputs and outputs to the 13 rules are seen to be somewhat sparse. This occurs because the inputs are utilized to achieve rather different goals. The first four rules are used to guide the output sign depending on the previous outcome and are useful in tracking the time variations. Rules 5 through 9 provide rapid convergence from a variety of larger initial error conditions. Rules 10-12 are relating the output magnitude to the absolute yoyo amplitude: "if there's not much yoyo then don't change anything very much". Rule 13 is a safety valve which deals with highly overcompensated cases by quickly reducing the DBA level and dominates other rules in the process.

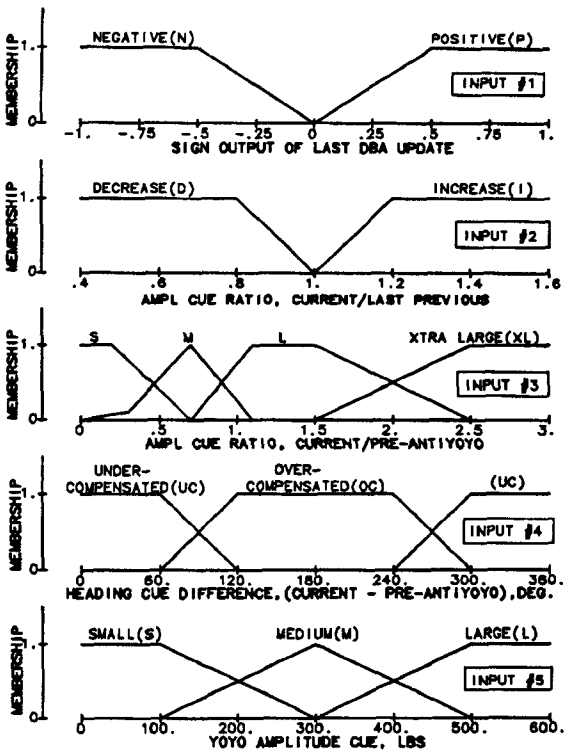

FIGURE 11

INPUT VARIABLE MEMBERSHIP FUNCTIONS -- FUZZY CONTROL -- DELTA BANK ANGLE(DBA) UPDATE

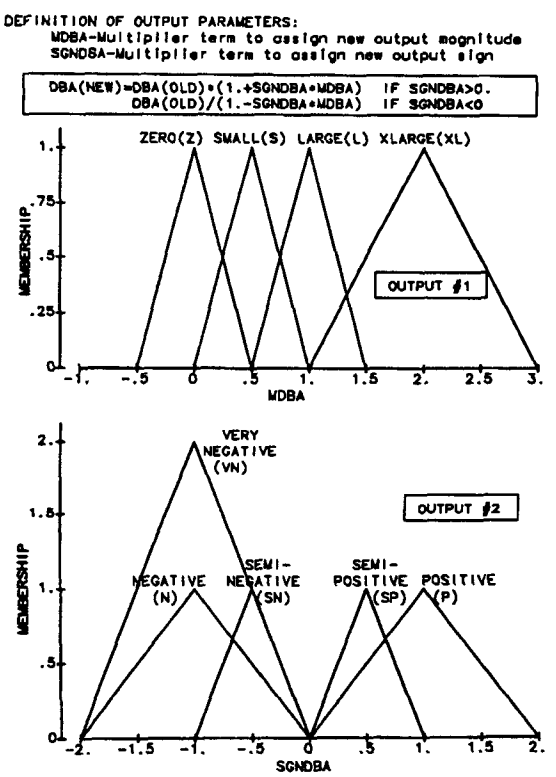

FIGURE 12

OUTPUT VARIABLE MEMBERSHIP FUNCTIONS -- FUZZY CONTROL -- DBA UPDATE

TABLE 1- RULE SET--FUZZY CONTROLLER--DELTA BANK ANGLE UPDATE CALCULATION

	INPUTS					OUTPUTS	
	IF	AND	AND	AND	AND	THEN	AND
RULE NO.	INPUT1	INPUT2	INPUT3	INPUT4	INPUT5	OUTPUT1	OUTPUT2
1	N	D	-	-	-	-	SN
2	P	D	-	-	-	-	SP
3	N	I	-	-	-	-	SP
4	P	I	-	-	-	-	SN
5	-	-	S	-	-	Z	-
6	-	-	M	-	-	S	-
7	-	-	L	-	-	L	-
8	-	-	NXL	UC	-	-	P
9	-	-	-	OC	-	-	N
10	-	-	NXL	-	S	Z	-
11	-	-	NXL	-	M	S	-
12	-	-	NXL	-	L	L	-
13	-	-	XL	-	-	XL	VN

Since the OLC maneuver is expected to converge moderately close to the optimum solution almost immediately, the high amplitude memberships("L", "XL", etc) and the rules they apply to are not normally active. The small corrections required following the OLC maneuver should primarily use rules 5,6,8-11.

Results

Flight test and simulation results have demonstrated that either of the anti-yoyo maneuver profiles of Figure 4, with the proper selection of RHA and DBA, are capable of reducing the yoyo amplitude to a very low level. The results shown here are from the auto-orbit simulation. Figure 13 shows the LTWA tension time response for a severe wind shear condition. After four orbits the LTWA has "dropped in" to a downward spiral orientation and the cues are close enough to steady state to be accurate yoyo indicators. The OLC anti-yoyo maneuver parameters are DBA=4.8 degrees and RHA=122.4 degrees. The optimum parameters, determined from other simulation runs, are 6.4 degrees and 122.5 degrees, respectively. Thus, the yoyo is significantly reduced by the OLC maneuver, but not quite optimum. Subsequent updates by the closed loop controller approach the optimum values.

To test the ability of the closed loop system to recover from severe error conditions, a large intentional error was substituted for the OLC maneuver. The response is shown in Figure 14. The RHA error was chosen to be almost 180 degrees away from the optimum. Thus, several large updates were required to reach the optimum. During this time, the cue amplitude value remained at a high level until the "bucket" shown in Figure 7(a) was reached. The important result is that the closed loop controller was able to utilize the large error to calculate the appropriate changes in the anti-yoyo parameters to achieve optimum values. While this large an error is not expected to occur in a normal scenario, the updates calculated by the fuzzy controller lead to a successful recovery.

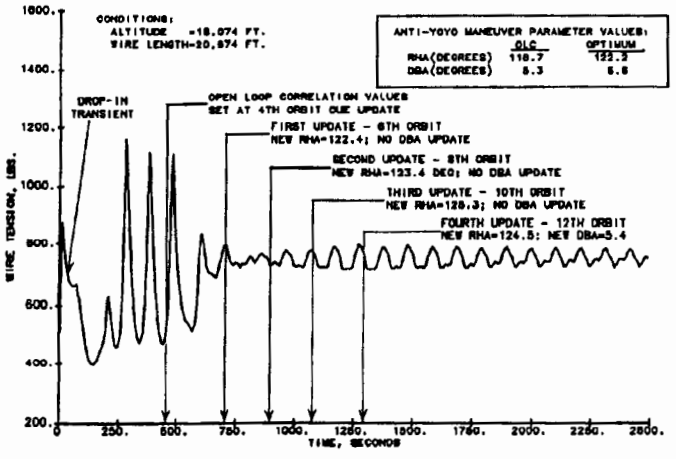

FIGURE 13
TRANSIENT RESPONSE -- ANTI-YOYO MANEUVER WITH OPEN LOOP CORRELATION(OLC)

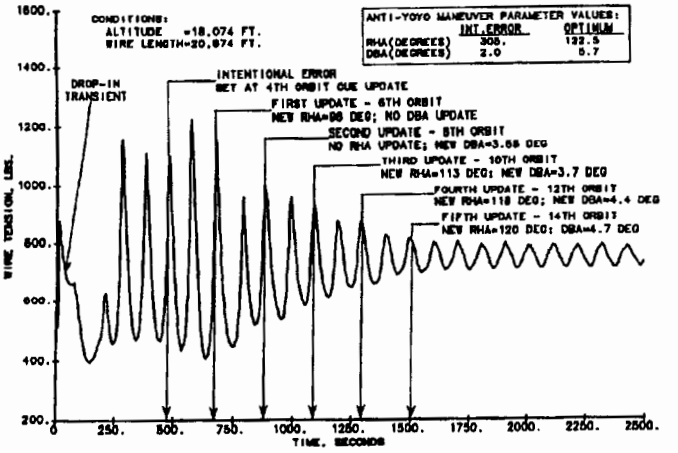

FIGURE 14
TRANSIENT RESPONSE - ANTI-YOYO MANEUVER WITH LARGE INTENTIONAL ERROR

Conclusions

An LTWA model and fuzzy logic control algorithm were developed and evaluated using a simulation. The model was validated by comparing it against flight test data with excellent agreement. The closed loop control system, using fuzzy logic constructs, was very effective in suppressing the LTWA yoyo oscillation. Fuzzy logic was found to be easy to tune and optimize for this control application.

Future effort will involve integrating the algorithm into the E-6 aircraft to permit fully automatic orbital flight. This will result in improved mission performance and reduced pilot workload.

Acknowledgements

The authors of this paper thank the many individuals who supported this effort. Special thanks to Boeing engineers: Mike Mock, Mike Smyth, and Colin Wiel; Boeing managers: Norm Bialek, Paul Collins, and Chris Sales; Navy representatives: Captain Ed Hampshire, Commander Tom Salacka, Lieutenant Pat Laird, Mr. Pat Eng, Mr. Curt Rosenbery, and Dr. Lou Schmidt. Special thanks to Jody Jinneman and Scott Seagren for their assistance in the preparation of this paper.

References

[1] Zadeh,L.,"Fuzzy Sets", *Information and Control*, VOL. 8, 1965, pp. 338-353.

[2] Kosko,B., *Neural Networks and Fuzzy Systems*, Englewood Cliffs, NJ, Prentice Hall, 1990.

[3] Omron Electronics, Inc., *Fuzzy Logic, A 21st Century Technology*, 1991.

[4] Berardinis,L., "Clear Thinking on Fuzzy Logic", *Machine Design*, April 23, 1992, pp. 46-52.

[5] Hoerner,S., *Fluid Dynamic Drag*, 1965, Ch. 3, p.11.